

AD



AD 635352

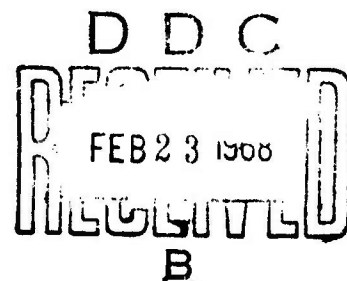
Technical Report ECOM-2308

CLUTTER ATTENUATION ANALYSIS

by

William Fishbein
Stanley W. Graveline
Otto E. Rittenbach

March 1967



ECOM

UNITED STATES ARMY ELECTRONICS COMMAND • FORT MONMOUTH, N.J.

DISTRIBUTION OF THIS DOCUMENT IS UNLIMITED

Reproduced by the
CLEARINGHOUSE
for Federal Scientific & Technical
Information Springfield Va 22151

ACQUISITION FOR	
CESTI	WRITE SECTION <input checked="" type="checkbox"/>
DDC	DIFF SECTION <input type="checkbox"/>
U. ANNOUNCED <input type="checkbox"/>	
CLASSIFICATION	
DISTRIBUTION/AVAILABILITY CODES	
DIST.	AVAIL. and/or SPECIAL
✓	

NOTICES

Disclaimers

The findings in this report are not to be construed as an official Department of the Army position, unless so designated by other authorized documents.

The citation of trade names and names of manufacturers in this report is not to be construed as official Government indorsement or approval of commercial products or services referenced herein.

Disposition

Destroy this report when it is no longer needed. Do not return it to the originator.

TECHNICAL REPORT ECOM-2808

CLUTTER ATTENUATION ANALYSIS

by

William Fishbein
Stanley W. Graveline
Otto E. Rittenbach

Radar Technical Area
Combat Surveillance and Target Acquisition Laboratory

March 1967

Subtask Nr. 1P6-20901-A-188-03-05

DISTRIBUTION OF THIS DOCUMENT IS UNLIMITED

UNITED STATES ARMY ELECTRONICS COMMAND . FORT MONMOUTH, NEW JERSEY

ABSTRACT

The performance of moving target indication (MTI) systems for combat surveillance radars depends to a large extent on the clutter spectrum. The clutter spectrum is especially important when the radar attempts to detect slowly moving ground targets. This spectrum has long been assumed to be Gaussian shaped. However, MTI system performance predicted by this assumption was not achieved in practice. This report describes the results of an investigation conducted to determine the performance to be expected from an MTI system.

The approach was to measure the clutter rejection ratios afforded by various high-pass filters. The signal was taken from the boxcar demodulator of an X-band radar observing different clutter targets under varying wind conditions. Clutter rejection ratios of 10 to 40 db were measured. These results were then used to obtain a theoretical expression for the clutter power spectrum. This expression differs from the usual Gaussian assumption. Some credence is given to the results by a direct spectral analysis performed on a clutter signal.

Two methods of filtering clutter signals which will result in acceptable MTI performance are suggested in this report.

The results of this investigation are significant in that they have led to establishing criteria for a better MTI system design.

CONTENTS

	Page
Abstract	11
INTRODUCTION	1
BACKGROUND	1
Video Processing	2
Filtering Need	2
Nature of a Clutter Target	2
CLUTTER ATTENUATION MEASUREMENTS	3
Clutter Rejection Ratio	3
Test Procedure	3
Clutter Spectrum Expression	5
GAUSSIAN COMPARISON	6
Gaussian Spectrum	6
Gaussian Comparison	6
SPECTRAL ANALYSIS	7
Procedure and Results	7
FILTER SUGGESTIONS	8
Conventional Filtering	8
Narrow Band Filtering	9
CONCLUSIONS	10
RECOMMENDATIONS	10

FIGURES

1. Setup for Measuring Clutter Rejection Ratios	11
---	----

CONTENTS (Contd.)

FIGURES	Page
2. f_c vs V , f_c = Characteristic Frequency of the Clutter Spectrum Obtained with an X-Band Radar	12
3. Approximations of the Clutter Spectra Obtained with an X-Band Radar: Wind Velocity 20 Knots	13
4. Approximations of the Clutter Spectra Obtained with an X-Band Radar: Wind Velocity 12 Knots	14
5. Approximations of the Clutter Spectra Obtained with an X-Band Radar: Wind Velocity 12 Knots	15
6. Clutter Rejection Ratios Obtained with 12 db/Octave High-Pass Filters	16
7. 12 db/Octave Active High-Pass Filter	17
8. Block Diagram of a Clutter-Controlled Range-Gated Filter Channel	18
III-1. Frequency Response Curves of Clutter Filters	23

TABLES

I. Clutter Filter Characteristics	4
II. Measured Clutter Rejection Ratios	4
III. Comparison of Measured and Calculated Clutter Rejection Ratios	5
III-1. Calculated Clutter Rejection Ratios	24

APPENDICES

I. A Video Processor	19
II. Characteristics of Radar Set AN/TPS-25	20
III. Clutter Rejection Ratio Computations	21
IV. Cubic and Gaussian Spectra Comparison	25

CONTENTS (Contd)

	Page
APPENDICES	
V. Clutter Rejection Ratio Calculation for a Gaussian Spectrum	27
REFERENCES	30

CLUTTER ATTENUATION ANALYSIS

INTRODUCTION

The purpose of MTI systems for combat surveillance radars is to process the radar video output to eliminate all undesired signals and have an output only for moving target input signals. The primary source of undesired signals which limit the performance of an MTI system is the spectrum resulting from wind blown natural clutter targets. A problem arises in that this spectrum contains doppler frequencies which overlap those resulting from slowly moving targets of interest, e.g., a walking man.

The clutter spectrum was long assumed to be Gaussian shaped. However, MTI system performance predicted by this assumption was not achieved in practice. An investigation was conducted to determine the system performance to be expected. This investigation led to the establishment of criteria for a better MTI system design.

The approach used was to measure the clutter rejection ratios afforded by various high-pass filters. The clutter signal was taken from the boxcar demodulator of an X-band noncoherent radar observing different clutter targets under varying wind conditions. A theoretical expression for the clutter spectrum was obtained from these data. The results of a direct spectral analysis performed on a clutter signal gave some credence to the theoretical expression obtained from the measurements. Comparisons with a Gaussian clutter spectrum were made and the error obtained with this assumption was calculated.

This report discusses the results of the investigation and the significance of the results.

BACKGROUND

An important function of certain combat surveillance radars is to provide information which will enable one to distinguish between fixed and moving ground-based targets. These radars are designed to make use of the doppler effect, i.e., to have as an output a signal which contains the frequencies resulting from target motion.

The most prevalent class of radar in use for combat surveillance is a pulse doppler noncoherent system. Noncoherent means that a fixed target reference must exist within the same range resolution cell as a moving target if moving target information is to be recovered. The output signal of such a radar is a video pulse train amplitude modulated according to the doppler frequency. The doppler modulation can be recovered by means of a circuit called

a boxcar demodulator. The boxcar is a sample-and-hold device, usually gated at the radar pulse repetition frequency. The boxcar output contains the doppler frequency. This audio signal is processed and fed to an indicator. The indicator in many MTI combat surveillance radars is a simple aural display. An operator notes the presence of a moving target by the sounds he hears.

Video Processing

While the operator does an excellent job of detecting moving targets, he can observe only a small area at a time. To increase the information rate of a radar and also to reduce operator fatigue, modern radar systems employ video processors.* A video processor provides an output only for moving target input signals in a form suitable for a visual display. This is accomplished by recovering the doppler frequencies via a boxcar demodulator, filtering to remove all undesired frequencies, rectifying, integrating, and gating the remaining signal. The final output is a video pulse occurring at the correct range.

Filtering Need

The basic sources of undesired frequencies that must be eliminated (or at least reduced) in the video processor are the returns from wind blown natural clutter targets. Conventional processors employ high-pass filters for this task. These filters must be critically designed. One which gives maximum MTI sensitivity on calm days would be ineffective on windy days. On the other hand, a filter that eliminated all clutter signals on a windy day would result in a needless loss of information on calmer days. A compromise is needed if this type of filtering is used. The nature of the clutter target suggests that a different type of filtering might be employed. The clutter analysis described in this report yields the information required to arrive at some filter design suggestions.

Nature of a Clutter Target

Foliage is the primary cause of doppler signals that compete with those from slowly moving targets in an MTI receiver. The detection cell size of a radar at a typical operating range might be 75 meters in both range and azimuth. If an area fairly dense in trees were under observation, the clutter return would consist of a complex addition of the returns from several trees. The total return will consist of a large d-c component plus a fluctuating component. The d-c return is due to the trunks of the trees and the large branches (plus any other fixed targets that fall within the detection cell). The a-c component is due to many small individual scatterers. These are the leaves and small branches of the trees. The a-c component varies according to the wind conditions.

* See Appendix I

CLUTTER ATTENUATION MEASUREMENTS

The original effort in this work was to experimentally determine the performance of various high-pass filters in attenuating clutter signals. The procedure used was to measure the clutter rejection ratios afforded by five filters when attenuating the signal provided by a radar observing several different clutter targets.

Clutter Rejection Ratio

A method of describing the performance of a filter in attenuating clutter signals is by its clutter rejection ratio. This is defined as:

R = Clutter Rejection Ratio

$$R = \frac{\int_0^{\infty} P(f) df}{\int_0^{\infty} P(f) |H(p)|^2 df} \quad (1)$$

where $P(f)$ = clutter power spectrum

$H(p)$ = filter voltage transfer function.

R is thus the ratio of the total clutter power into the filter to the total power out.

Test Procedure

The clutter rejection ratios of five high-pass filters were obtained by means of an extensive series of measurements. An AN/TPS-25 radar system* was used to collect data for the measurements. This radar is of the noncoherent pulse doppler type. It operates at a 3-cm wave length (X-band). Target information was taken from the boxcar demodulator output of the radar. This output contains the clutter spectrum when the radar is observing a natural clutter site.

Figure 1 is a block diagram of the experimental equipment used. The radar boxcar output was fed into five parallel filter channels and a reference channel. The filter output was amplified, rectified, and integrated via a thermocouple, chopped, and fed into a pen recorder. The thermocouple output was chopped to eliminate any errors due to bias drifts and to provide a more sensitive input to the pen recorder. The output of each filter channel was compared with the output of the reference (unfiltered) channel on the recorder. The ratio of these two values is the clutter rejection ratio.

The high-pass filters** for which clutter rejection ratios were measured are described in Table I below.

* Characteristics of Radar Set AN/TPS-25 are given in Appendix II.

** Frequency response plots of the filters are given in Appendix III.

TABLE I
CLUTTER FILTER CHARACTERISTICS

ATTENUATION SLOPE db/octave	CUTOFF FREQUENCY Hz	TYPE
6	50	passive
6	100	passive
12	100	active
40	50	passive
40	100	passive

Six different clutter targets were observed by the radar. The range to the targets was always such that many trees fell within the radar detection cell. The procedure used was to measure the clutter rejection ratio (R) obtained with each filter when operating on the spectrum provided by a particular clutter site. Observations on different days provided a value of R as a function of the wind conditions to which each target was subjected. Finally, the rejection ratios obtained with the six targets were averaged. The results are summarized in Table II below.

TABLE II
MEASURED CLUTTER REJECTION
RATIOS

	50	100	100	50	100	← f_p
V	6	6	12	40	40	← α
3	24	26	37	36	40	} R
6	21	26	36	33	38	
9.5	17	17	30	27	34	
13.5	15	18	26	-	29	
18	11	16	21	-	23	
20	9	13	18	-	19	

f_p = Filter low-frequency cutoff (Hz)

α = Filter attenuation per octave below f_p (db)

V = Average wind velocity (knots)

R = Clutter rejection ratio (db)

Clutter Spectrum Expression

An attempt was made to find an expression for the clutter power spectrum which would yield calculated values for the clutter rejection ratio in agreement with Table II. An expression that gives good agreement is

$$P(f) = \frac{1}{1 + \left(\frac{f}{f_c}\right)^3} \quad (2)$$

where f_c = clutter spectrum characteristic frequency

$$= k \exp [\beta V] \text{ (Hz)} \quad (3)$$

$$k = 1.33 \text{ (Hz)}$$

$$\beta = 0.1356 \text{ (knots)}^{-1}$$

V = wind velocity (knots) .

The expression for f_c is plotted in Figure 2. Calculated values* of R using (2) and (3) are compared with the measured values in Table III below.

TABLE III
COMPARISON OF MEASURED AND CALCULATED
CLUTTER REJECTION RATIOS

		50		100		100		50		50		f_p
		6		6		12		40		40		α
V	f_c	M	C	M	C	M	C	M	C	M	C	R
3	2	24	24	26	29**	37	38	36	35	40	41	
6	3	21	21	26	26	36	35	33	31**	38	38	
9.5	5	17	17	17	22**	36	30	27	27	34	33	
13.5	8	15	14	18	19	26	26			29	29	
18	15	11	10	16	15	21	21			23	24	
20	20	9	9	13	13	18	19			19	21**	

f_p = filter low-frequency cutoff (Hz)

α = filter attenuation per octave below f_p (db)

V = average wind velocity (knots)

f_c = clutter spectrum characteristic frequency (Hz)

R = clutter rejection ratio (db)

M = measured value

C = calculated value

** denotes a difference of more than one db between the measured and calculated values.

* See Appendix III

It can be seen in the table that, of 27 values compared, 23 differ by one db or less. Two of the remaining four differ by 2 db. The measured and calculated values are thus seen to be in very good agreement.

The results of the experimental program are summarized by Equations (2) and (3). The performance of any filter in attenuating the clutter spectrum provided by an X-band radar can be predicted from these expressions.

GAUSSIAN COMPARISON

The clutter spectrum has long been assumed to be Gaussian shaped. However, MTI system performance predicted by this assumption was not achieved in practice. A comparison will be made here between the cubic power spectrum described by Equation (2) and the long assumed Gaussian spectrum.

Gaussian Spectrum

Kerr¹ and Barlow², in early work, stated that the power spectrum of fluctuating clutter targets can be approximated by

$$P(f) = \exp \left[-af^2 \right] \quad (4)$$

where a = a constant determined by the type of target, radar frequency, and wind conditions (sec^2).

Skolnik³ quotes a value of $a = 2.3 \times 10^{-3}$ for the spectrum obtained with a radar operating at a frequency of 10 GHz observing a heavily wooded area subjected to a wind velocity of 20 mph.

Gaussian Comparison

One method of comparing the spectra described by Equations (2) and (4) is to assume that the two spectra have equal total powers. Then*

$$\int_0^{\infty} \frac{df}{1 + \left(\frac{f}{f_c}\right)^3} = \int_0^{\infty} \exp \left[-af^2 \right] df$$

$$\text{and } f_c = \frac{3}{4} \left[\frac{3}{\pi a} \right]^{1/2}. \quad (5)$$

Substituting the value of a given above into Equation (5) results in an f_c of 15.3 Hz.

It is to be noted that a value for f_c of 14 Hz can be found from Equation (3) for a 20 m.p.h. (17.4 knot) wind. This is in good agreement with the 15.3 Hz value when one considers the two were obtained through completely

* See Appendix IV

independent investigations. For this comparison, f_c is taken equal to 15.3 Hz. The two spectra are plotted in Figure 3. The curves are seen to be similar. The main difference is that the Gaussian spectrum decays more quickly beyond 30 Hz. This difference is emphasized by comparing the clutter rejection ratios obtained when the spectra are attenuated by 12-db-per-octave active 100-Hz high-pass filters. R for the Gaussian case is calculated (Appendix V) to be 28.5 db. From Table II, R for the cubic spectrum is seen to be 21 db. The 7.5 db difference is attributed to the difference in energy available in the two spectra at the higher frequencies. It is seen then that assumption of a Gaussian spectrum gives a more optimistic prediction of clutter attenuation and thus MTI performance than is actually achieved. The difference in the rejection ratios increases with increasing wind conditions.

SPECTRAL ANALYSIS

The process described up to this point has been to measure the clutter attenuation afforded by various filters and then find a theoretical expression for the clutter spectrum based on these measurements. One might ask why a different approach was not used, i.e., why not perform a direct analysis on a clutter signal? This would yield the clutter power spectrum from which the performance of the selected filters could be determined. The answer to the question of methods is that filter performance can be determined with significantly less effort by making attenuation measurements. A spectral analysis would result in meaningful data only after many clutter samples were observed for lengthy intervals. An extensive analysis on these samples would then have to be made; finally, the attenuation afforded by the various filters would have to be calculated.

A spectral analysis for the clutter return from a single target and single wind condition was performed in an attempt to verify the cubic clutter power spectrum expression derived previously.

Procedure and Results

The boxcar demodulator output of the radar was recorded while the radar was observing a clutter target subjected to a wind velocity of 12 knots. A one second length of the recording was sampled 200 times ($\Delta t = 5$ milliseconds). A computer was programmed to determine the power spectrum via a direct Fourier analysis.⁴

The power spectra for six one-second samples of the recorded clutter data were obtained. A mean was taken of the six values for each frequency. The data points are plotted in Figure 4. A plot of the spectrum for a 12-knot wind given by Equations (3) and (4) is also shown in Figure 4. The question is, how well does the curve fit the data points? The curve is seen to be a good approximation above 10 Hz. In fact, above 20 Hz, the curve is probably the best possible approximation to the data points.

The good agreement between the data points and the curve at the higher frequencies gives strong credence to the accuracy of assuming a cubic clutter spectrum. Also plotted in Figure 4 is a Gaussian-shaped spectrum having the same total power as the cubic spectrum. It can be seen that this curve is a

poorer approximation for the data points at the higher frequencies. A linear plot of the two curves is seen in Figure 5. It again shows the similarity between the two curves, the main difference being that the Gaussian spectrum decays more quickly.

FILTER SUGGESTIONS

The results obtained up to this point can now be used to suggest filters which will give satisfactory performance in an MTI video processor. What is sought is a filter which will sufficiently attenuate clutter signals with a minimum loss of signals from slowly moving targets of interest. The clutter filter may be repeated up to a few hundred times in some video processors. This fact dictates that the filter be of simple design in order that resulting sizes and weights be reasonable.

Two types of filtering are discussed in the sections that follow.

Conventional Filtering

Typical video processors (Appendix I) employ high-pass filtering to reduce signals resulting from clutter targets. A filter having a clutter rejection ratio of at least 20 db will usually give satisfactory MTI performance. An active filter with an attenuation slope of 12 db per octave meets this requirement. The clutter rejection ratios afforded by these types of filters having cutoff frequencies of 50 and 100 Hz are plotted in Figure 6. The rejection ratios for the 50-Hz filter were calculated; those of the 100-Hz filter are repeated from Table II. The rejection ratio provided by the 50-Hz filter is greater than 20 db for wind velocities up to 10 knots. The 100-Hz filter provides an attenuation of at least 20 db for nearly all wind conditions.

A circuit diagram of the active filter is shown in Figure 7. It contains two active and six passive elements. The two transistors may be replaced by a single high input impedance device such as a field-effect transistor. The filter can be packaged so that its contribution in size and weight compared to that of an overall MTI system is small.

The active elements in the filter sharpen the break point of the frequency response of the filter, also shown in Figure 7. The filter attenuates an input signal at a frequency of $f/f_p = 1$ by less than 1 db; a passive dual RC filter, while having the same attenuation slope as the active filter for $f/f_p \ll 1$, would attenuate a signal by 6 db at the break point. The sharp break point allows a good approximation of the frequency response of the active filter, e.g.

$$\begin{aligned} |H(f)| &= \left(\frac{f}{f_p}\right)^2, & f \leq f_p \\ &= 1, & f > f_p. \end{aligned}$$

The filter has no insertion loss in the pass band.

Because of its simplicity, small size and weight, and performance, a 12-db-per-octave active filter has been selected for use in several MTI systems. A filter having a cutoff frequency of 50 Hz is used in most applications; one system offers a choice between a 50-Hz and a 100-Hz cutoff. The 50-Hz cutoff is preferred, since it allows a greater range of target frequencies to pass.

A 6-db-per-octave passive filter having a cutoff frequency of 100 Hz also meets the requirements of performance and simplicity. However, the 50-Hz active filter discussed above is preferred because of its lower cutoff frequency. A 6-db-per-octave passive filter does not provide sufficient clutter attenuation.

Although the 40-db-per-octave filter meets attenuation requirements, the complexity of the filter circuit results in excessive size and weight.

Narrow Band Filtering

The preceding section indicates that a 12-db-per-octave active filter with a cutoff frequency of 50 Hz will give adequate performance in an MTI video processor. This filter still has the basic limitation that its frequency response is fixed while the signal it is designed to attenuate, i.e., the clutter spectrum, varies significantly according to the wind conditions to which the clutter target is subjected. On a calm day, the suggested filter would do a good job in eliminating clutter signals. For a calm condition, it would be possible (and desirable) to lower the cutoff frequency of the filter to allow a greater range of target frequencies to pass. On windy days, i.e., with winds above 10 knots, the filter will not provide sufficient clutter attenuation. It would be desirable under these conditions to raise the cutoff frequency of the filter.

A method of overcoming the limitations imposed by a single high-pass filter is to divide the entire audio bandwidth over which frequencies resulting from any target motion occur into several narrow band filters. This scheme allows the gain of the lower frequency bands to be adjusted according to the clutter conditions. A further improvement would be a system in which the gain of the low frequency bands would vary simultaneously with changing clutter conditions. An example of how this might be accomplished is shown in Figure 8. The outside boxes in the block diagram illustrate the method by which doppler information is processed. The boxcar output contains clutter and target signals.

A narrow band filter follows an amplification stage; the purpose of this filter is to pass only target signals. After further processing, the signal is threshold detected. The threshold level might be set by the signal level out of a clutter sampler. The sampler could be a narrow band filter centered at a frequency below that of the target filter, i.e., the filter designed to pass target frequencies. Under calm conditions, little energy would enter the clutter sampler and the threshold level would be at a minimum level. As the wind increases, clutter signals will be passed by the target filter. However, the energy in the clutter sampler will also increase, thus raising the threshold level which a signal passed by the target filter must exceed. No output signal due to clutter signals will exist at the threshold detector output.

Use of this scheme will yield the maximum signal-to-clutter level allowable under all conditions, thus obtaining a considerable enhancement in the performance of MTI systems.

CONCLUSIONS

The clutter spectrum received by a noncoherent X-band radar observing a group of natural clutter targets can be approximated by

$$P(f) = \frac{1}{1 + \left(\frac{f}{f_c}\right)^3}$$

$$\text{where } f_c = k \exp \left[\beta v \right] \text{ Hz}$$

$$k = 1.33 \text{ Hz}$$

$$\beta = .1356 \text{ knots}^{-2}$$

$$v = \text{wind velocity (knots) .}$$

This equation is significant in that the performance of any filter in attenuating clutter signals can now be predicted. The cubic expression gives a more accurate prediction of filter performance than the long assumed Gaussian spectrum.

A 12-db-per-octave active high-pass filter having a cutoff frequency of 50 Hz will provide a clutter attenuation of at least 20 db for winds up to 10 knots, which will afford satisfactory MTI performance under most conditions.

MTI system performance can be improved by covering the audio spectrum with several narrow band filters. Applying adaptive filtering techniques to the lower frequency bands will result in the maximum MTI sensitivity possible under all wind conditions.

RECOMMENDATIONS

Future effort should be expended in three areas. Firstly, the variations in the clutter spectrum with changes in the operating frequency of the radar should be determined. The return from coherent radars should also be analyzed.

Secondly, work should be done in developing a suitable adaptive filtering technique to yield maximum MTI sensitivity.

Finally, a study should be made to see if moving target signals of interest can be separated from clutter signals by using the statistical properties of clutter.

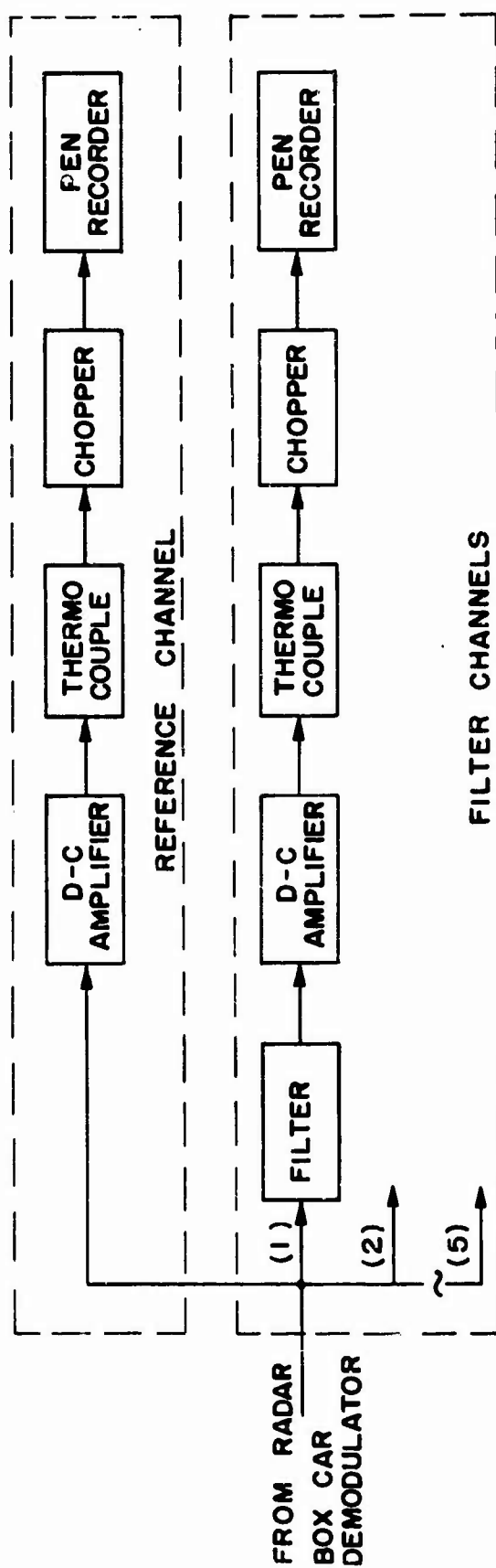


FIG. 1 SETUP FOR MEASURING CLUTTER REJECTION RATIOS

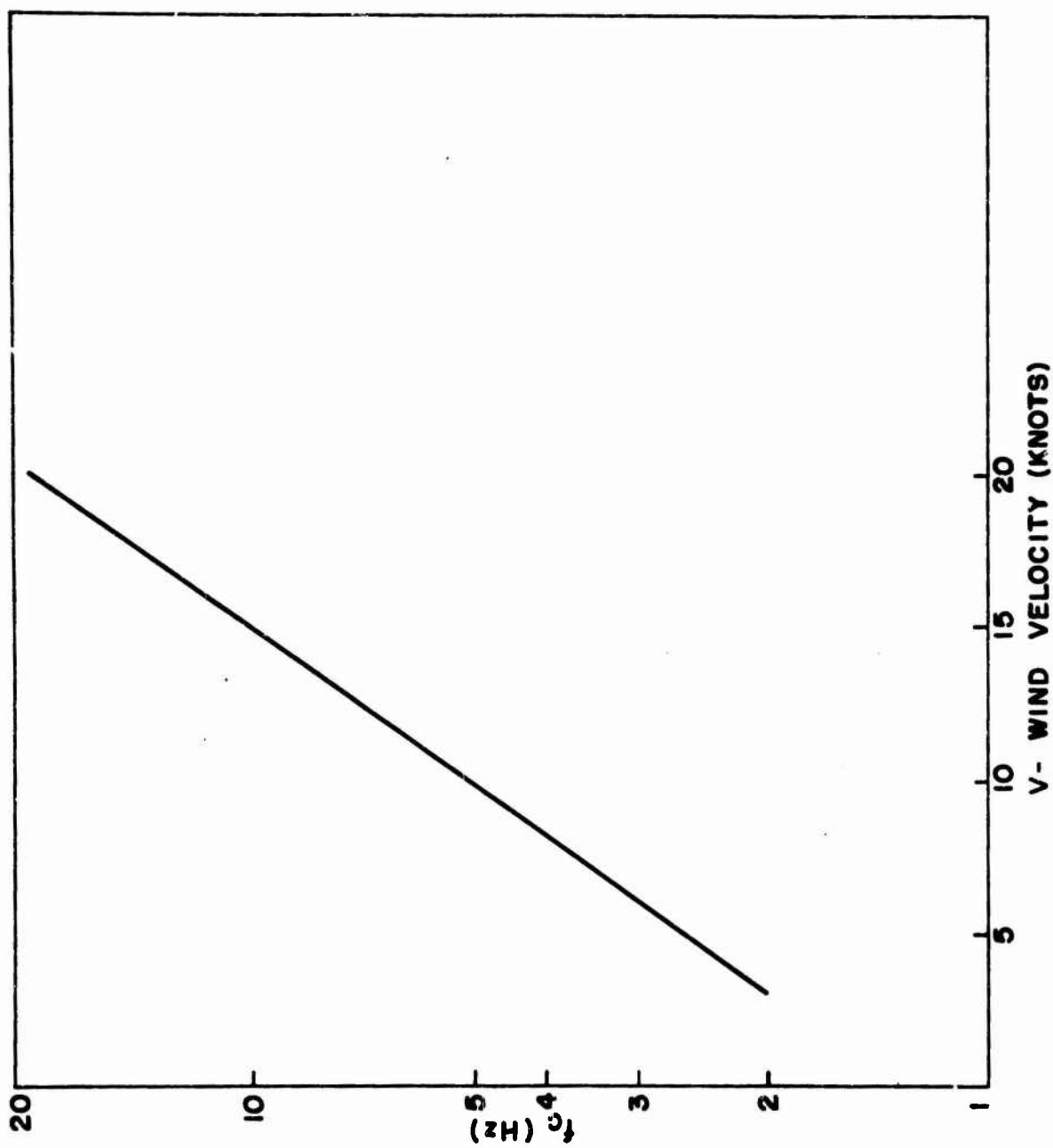


FIG. 2 f_c vs V , f_c = CHARACTERISTIC FREQUENCY OF THE CLUTTER SPECTRUM OBTAINED WITH AN X-BAND RADAR

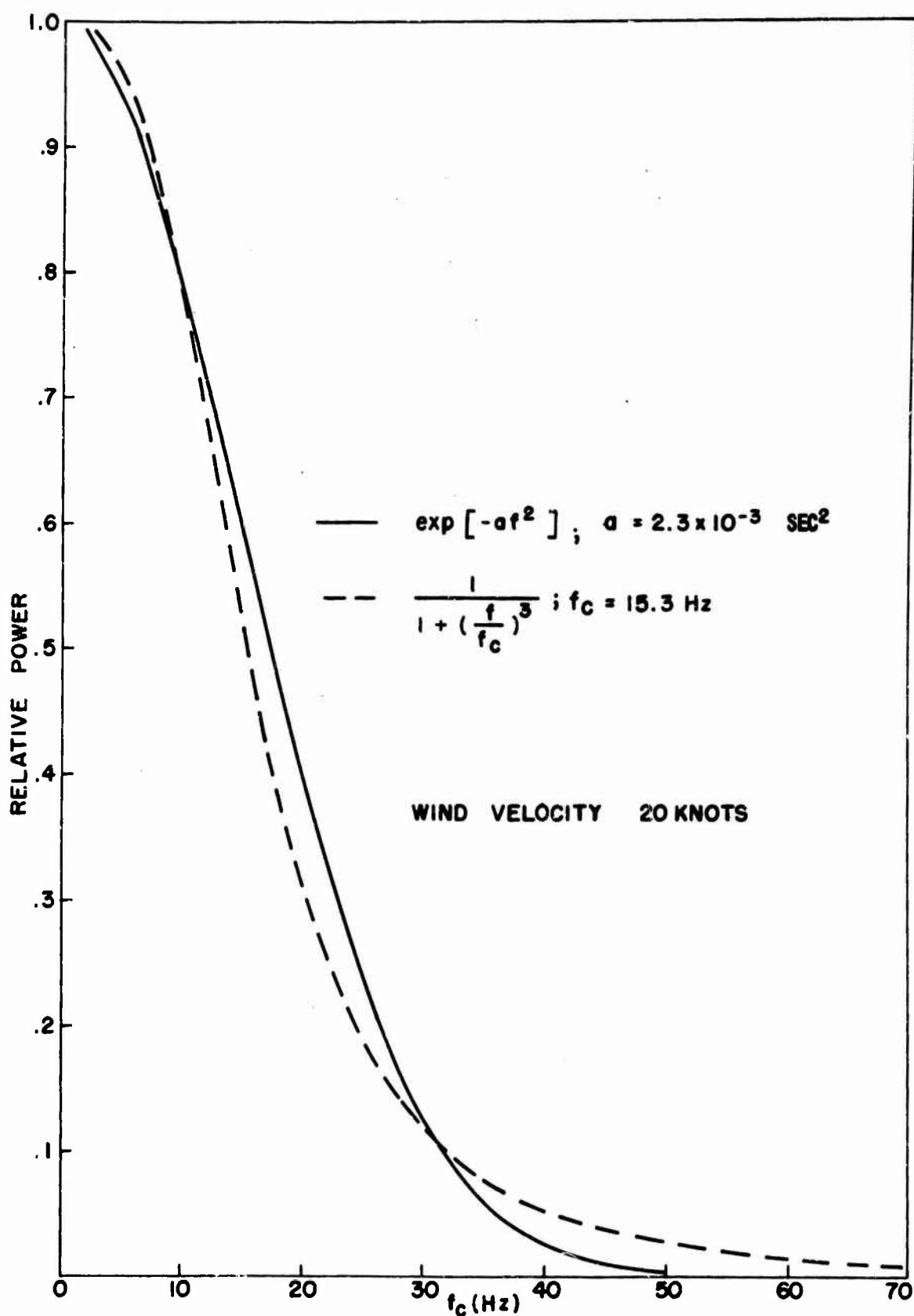


FIG. 3 APPROXIMATIONS OF THE CLUTTER SPECTRA OBTAINED WITH AN X-BAND RADAR

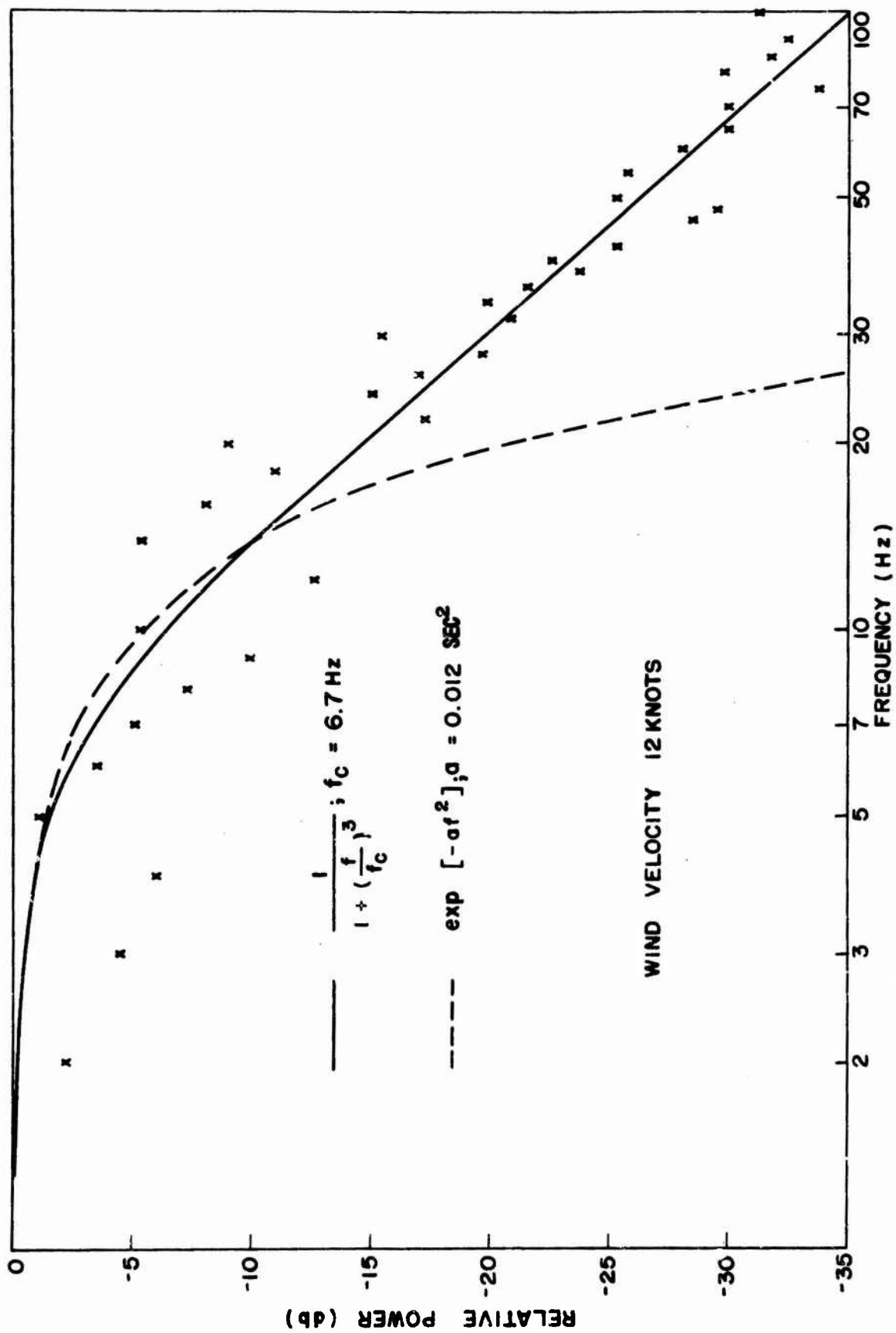


FIG. 4 APPROXIMATIONS OF THE CLUTTER SPECTRA OBTAINED WITH AN X-BAND RADAR

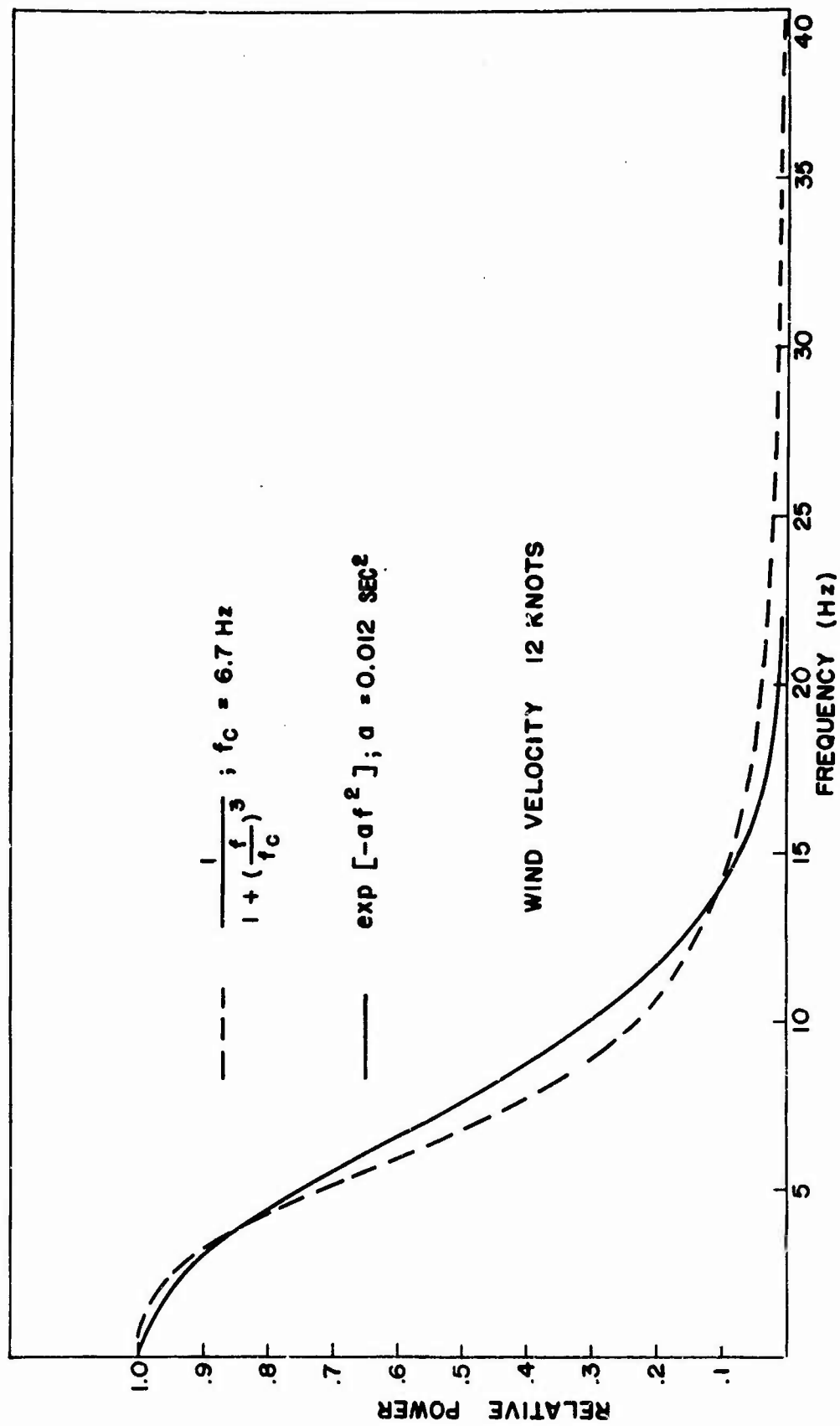


FIG. 5 APPROXIMATIONS OF THE CLUTTER SPECTRA OBTAINED WITH AN X-BAND RADAR

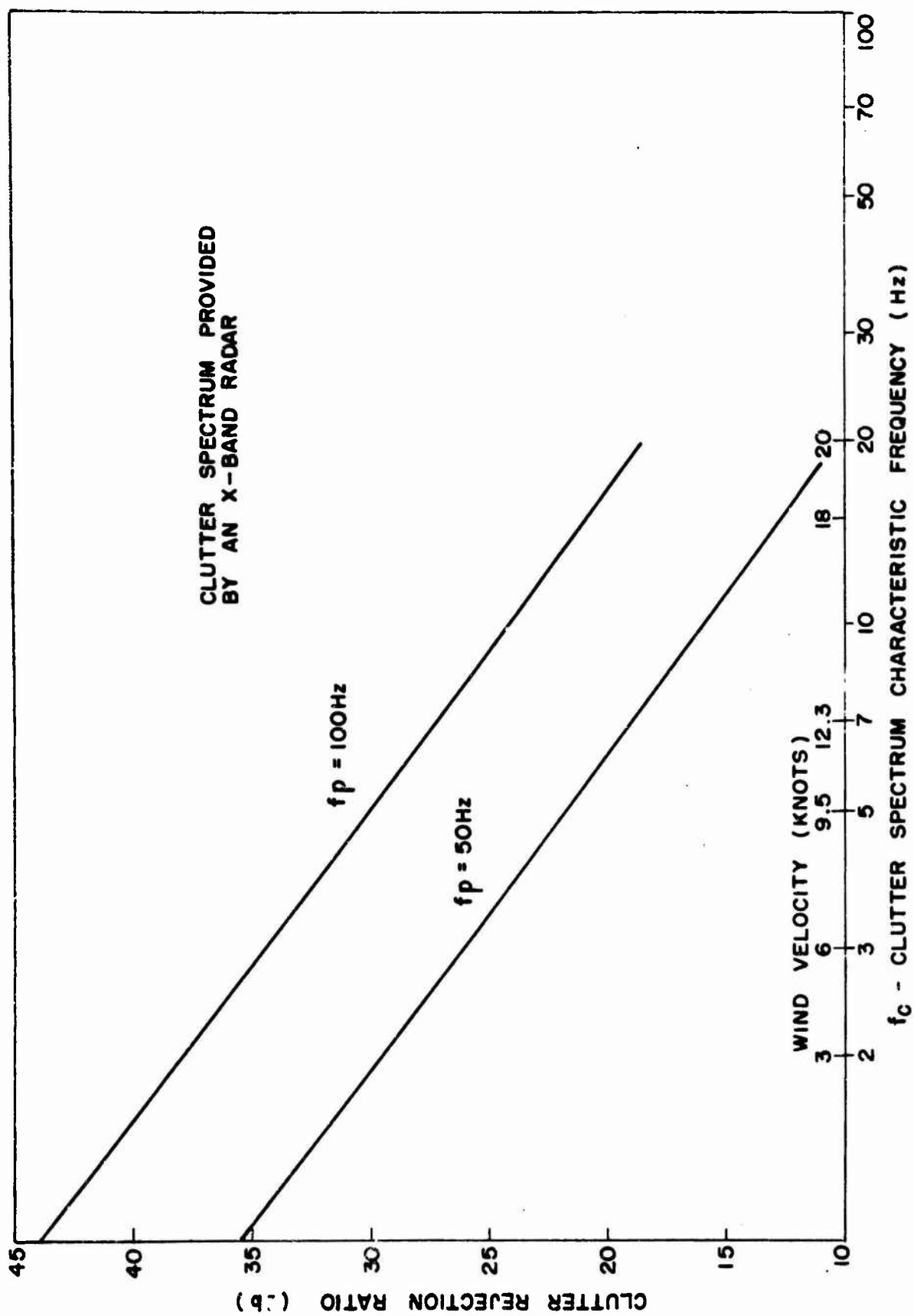


FIG. 6 CLUTTER REJECTION RATIOS OBTAINED WITH 12db/OCTAVE HIGH-PASS FILTERS

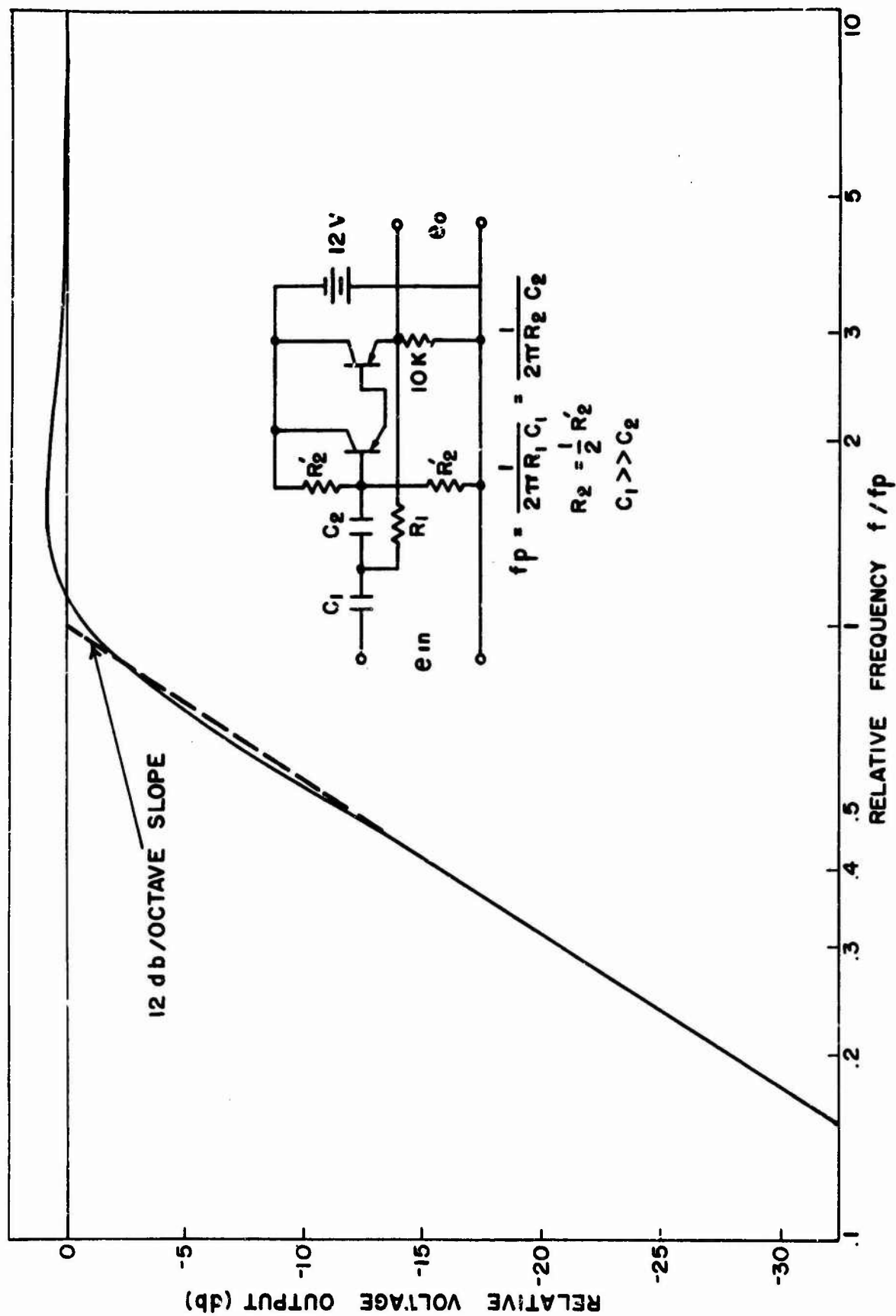


FIG. 7 12db/OCTAVE ACTIVE HIGH-PASS FILTER

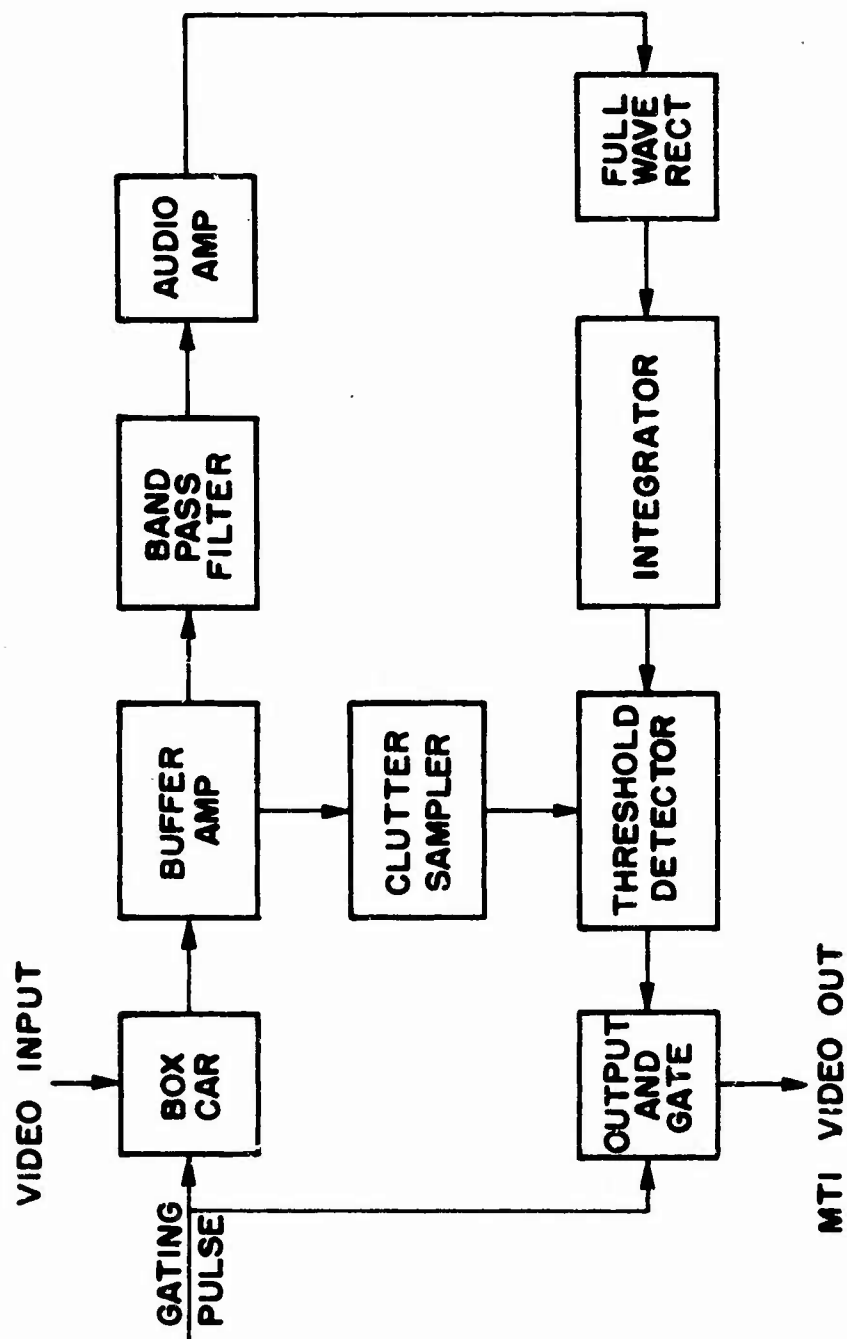


FIG. 8 BLOCK DIAGRAM OF A CLUTTER-CONTROLLED RANGE-GATED FILTER CHANNEL

APPENDIX I

A VIDEO PROCESSOR

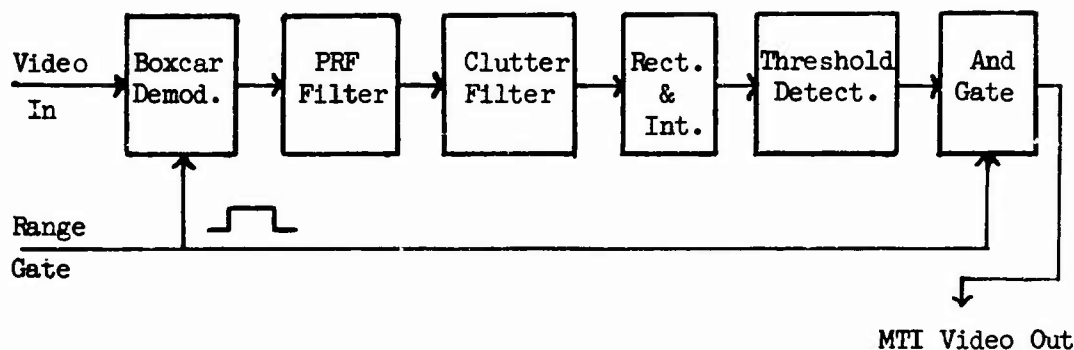


FIGURE I-1

RANGE-GATED FILTER CHANNEL

The basic building block of a video processor for pulsed radar systems is a range-gated filter channel. Figure I-1 shows a block diagram of a range channel. A boxcar demodulator is used to recover the doppler modulation information present in the video output of a radar system. The boxcar is a sample-and-hold device. It is usually gated at the radar PRF, with a pulse width equal to that of the transmitted pulse.

The delay of the gating pulse in relation to the transmitted pulse determines the range of the target being sampled. The boxcar output is a complex audio signal. Ambiguous signals, high frequency noise, and components of the PRF are removed by a low-pass filter. This filter has a high frequency cutoff of one-half the radar pulse repetition frequency. D-c signals resulting from fixed targets and other undesired low-frequency signals are eliminated by a high-pass filter. These latter signals result primarily from wind-blown natural clutter targets. The remaining signal is rectified, integrated, and threshold detected. The detector output is regated with the same pulse that gated the boxcar. The final output is a video pulse occurring at the correct radar range. A pulse will appear only for moving target inputs.

It is possible to use several range channels, each corresponding to a specific radar range interval. In this manner, moving targets appearing anywhere within the antenna beamwidth can be displayed simultaneously on a radar indicator.

APPENDIX II

RADAR SET AN/TPS-25 CHARACTERISTICS

The Radar Set AN/TPS-25 is a long-range noncoherent pulse doppler combat surveillance radar. The radar characteristics are as follows:

Frequency	9375 megahertz
Pulse Width	0.5 microseconds
PRF	1850 pulses per second
Peak Power	65 kilowatts
Azimuth Beamwidth	2 degrees
Elevation Beamwidth	4 degrees
Sector Scan	30 degrees in 22 seconds
Maximum Range	20,000 yards

APPENDIX III

CLUTTER REJECTION RATIO COMPUTATIONS

A method of calculating the clutter rejection ratios provided by various filters when attenuating the clutter spectrum is discussed here. The clutter rejection ratio is defined by

$R =$ Clutter Rejection Ratio

$$= \frac{\int_0^{\infty} P(f) df}{\int_0^{\infty} F(f) |H(P)|^2 df} \quad (\text{III-1})$$

where $P(f) =$ clutter power spectrum

and $H(P) =$ filter voltage transfer function.

The clutter spectrum can be approximated by

$$P(f) = \frac{1}{1 + \left(\frac{f}{f_c}\right)^3} \quad (\text{III-2})$$

where $f_c =$ clutter spectrum characteristic frequency (Hz).

The numerator of (III-1) can then be expressed as

$$\int_0^{\infty} \frac{df}{1 + \left(\frac{f}{f_c}\right)^3} .$$

This integral can be evaluated directly.

$$\text{Let } X = \frac{f}{f_c} .$$

Then

$$\int_0^{\infty} \frac{df}{1 + \left(\frac{f}{f_c}\right)^3} = f_c \int_0^{\infty} \frac{dx}{1 + x^3} .$$

The substitution $s = x^3$ results in

$$f_c \int_0^{\infty} \frac{dx}{1+x^3} = \frac{f_c}{3} \int_0^{\infty} \frac{s^{1/3-1}}{1+s} ds.$$

Evaluation of the right-hand integral requires the use of Beta and Gamma functions.⁶ The result is given in many handbooks of definite integrals. From Burlington,⁷

$$\int_0^{\infty} \frac{y^{n-1}}{1+y} dy = \frac{\pi}{\sin n\pi}, \quad 0 < n < 1.$$

Using this,

$$\int_0^{\infty} \frac{df}{1 + \left(\frac{f}{f_c}\right)^3} = \frac{2\sqrt{3}\pi f_c}{9}. \quad (\text{III-3})$$

The denominator of (III-1) cannot usually be evaluated by direct integration. Evaluation requires use of a form of the fundamental theorem of integral calculus,⁸ i.e.

$$\int_0^{\infty} P(f) |H(f)|^2 df = \lim_{\substack{N \rightarrow \infty \\ \Delta_f \rightarrow 0}} \sum_{n=1}^N P(f = n\Delta_f) |H(p = n\Delta_f)|^2 \Delta_f. \quad (\text{III-4})$$

For all clutter spectra and filters used to attenuate clutter signals, the values $\Delta_f = 1$ Hz and $N = 200$ are sufficient for the summation to be a good approximation to the integral.

The clutter rejection ratios of six filters acting on the clutter spectrum were obtained by programming a computer to perform the computations shown in Equations (III-3) and (III-4). Values of f_c , the clutter spectrum characteristic frequency, of from one to twenty Hz were taken in one Hz increment. Magnitudes of the filter transfer functions $H(p)$ were taken directly from frequency response plots of the filters. The plots are shown in Figure (III-1).

The calculated clutter rejection ratios are given in Table III-1.

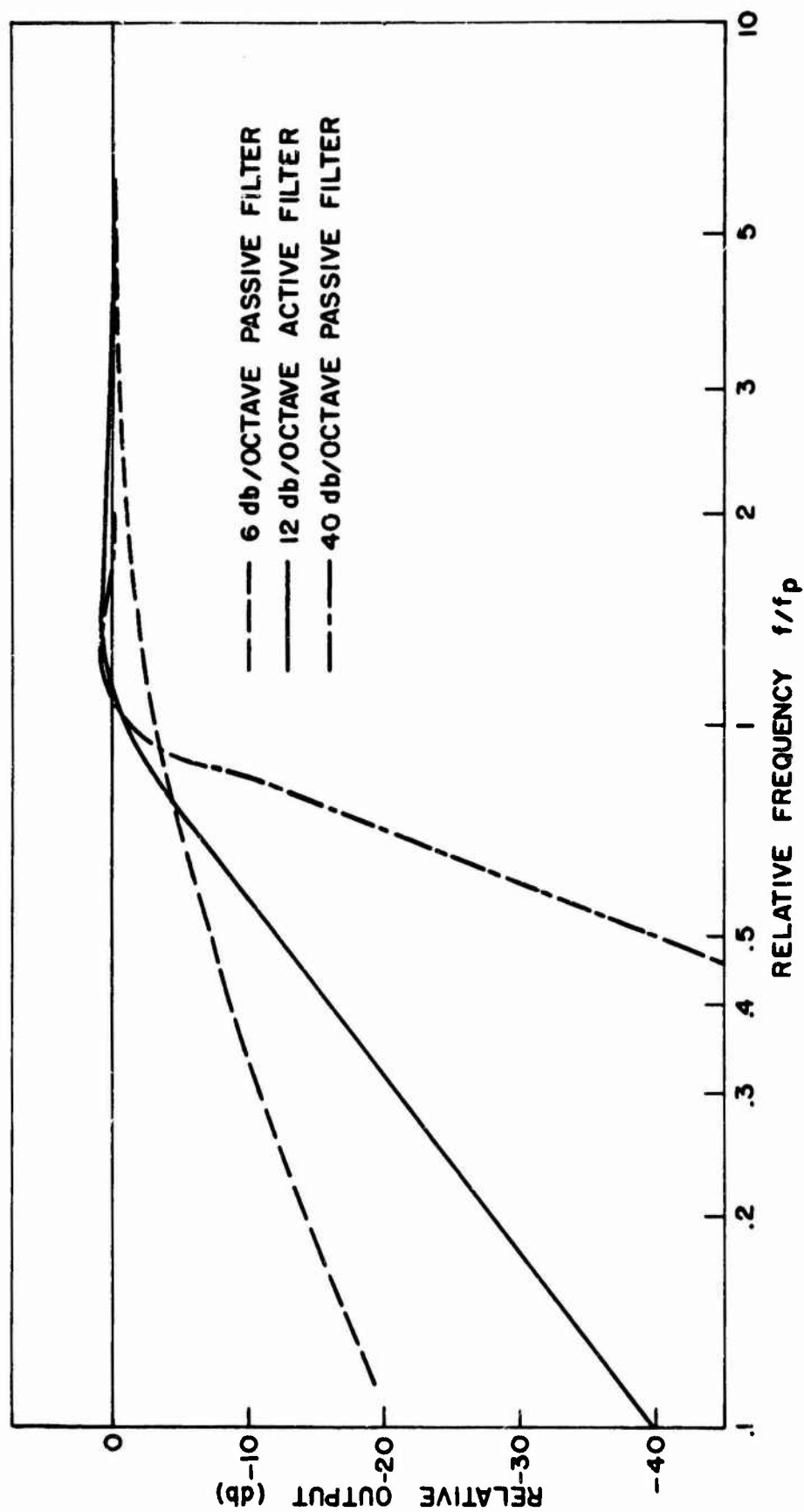


FIG. III-1 FREQUENCY RESPONSE CURVES OF CLUTTER FILTERS

TABLE III-1

CALCULATED CLUTTER REJECTION RATIOS

f_c (Hz)	50	100	50	100	50	100	f_p (Hz)
	6	6	12	12	40	40	α (db)
1	29	35	36	44	41	47	R(db)
2	24	29	30	38	35	41	
3	21	26	26	35	31	38	
4	19	24	24	32	29	35	
5	17	22	22	30	27	33	
6	16	21	20	29	25	32	
7	15	20	19	27	24	30	
8	14	19	18	26	23	29	
9	13	18	17	25	22	28	
10	13	17	16	24	21	27	
11	12	17	15	24	20	26	
12	12	16	14	23	19	26	
13	11	16	14	22	19	25	
14	11	15	13	22	18	24	
15	10	15	13	21	17	24	
16	10	14	12	20	17	23	
17	10	14	12	20	16	23	
18	9	13	11	19	16	22	
19	9	13	11	19	15	22	
20	9	13	10	19	15	21	

f_p = filter low-frequency cutoff

α = filter attenuation slope

f_c = clutter spectrum characteristic frequency

R = clutter rejection ratio

APPENDIX IV

CUBIC AND GAUSSIAN SPECTRA COMPARISON

Two approximations to the clutter power spectrum are

$$P(f) = \exp \left[-af^2 \right]$$

and
$$P(f) = \frac{1}{1 + \left(\frac{f}{f_c} \right)^3}$$

where a and f_c are constants determined by the frequency of the radar observing the clutter target and wind velocity to which the clutter target is subjected.

The constants a and f_c can be related by assuming that the two spectra have equal total powers. Then,

$$\int_0^{\infty} \frac{1}{1 + \left(\frac{f}{f_c} \right)^3} df = \int_0^{\infty} \exp \left[-af^2 \right] df. \quad (\text{IV-1})$$

The right-hand integral can be written as

$$\frac{\sqrt{2\pi}}{\sqrt{2a}} \int_0^{\infty} \frac{1}{\sqrt{2\pi}} \exp \left[-\frac{1}{2} (\sqrt{2a} f)^2 \right] \sqrt{2a} df.$$

This integral is the normalized Gaussian function and has a value of $1/2$.

$$\therefore \int_0^{\infty} \exp \left[-af^2 \right] df = \frac{\sqrt{\pi}}{2\sqrt{a}}.$$

The left-hand integral in IV-1 can be evaluated from tables of definite integrals.* The result is

$$\int_0^{\infty} \frac{df}{1 + \left(\frac{f}{f_c} \right)^3} = \frac{2\sqrt{3}\pi f_c}{9}.$$

* See Appendix III

Equating the results of these two integrals,

$$\frac{2 \sqrt{3} \pi f_c}{9} = \frac{\sqrt{\pi}}{2 \sqrt{a}}$$

$$\text{and } f_c = \frac{9}{4 \sqrt{3} \pi a} \cdot$$

APPENDIX V

CLUTTER REJECTION RATIO CALCULATION FOR A GAUSSIAN SPECTRUM

The clutter rejection ratio obtained when a 12-db-per-octave active high-pass filter attenuates a Gaussian-shaped clutter power spectrum is calculated here. The rejection ratio is defined by

$$R = \frac{\int_0^{\infty} P(f) df}{\int_0^{\infty} P(f) |H(p)|^2 df}$$

where $P(f)$ = clutter power spectrum

and $H(p)$ = filter voltage transfer function.

A Gaussian spectrum may be expressed by

$$P(f) = \exp \left[-af^2 \right]$$

where a is a constant determined by the frequency of the radar when observing the clutter target and wind velocity to which the clutter target is subjected.

A good approximation of the transfer function of a 12-db-per-octave high-pass filter is

$$\begin{aligned} H(p) &= \left(\frac{f}{f_p} \right)^2 & f \leq f_p \\ &= 1 & f > f_p \end{aligned}$$

where f_p is the filter cutoff frequency.

Then

$$R = \frac{\int_0^{\infty} \exp \left[-af^2 \right] df}{\int_0^{f_p} \left(\frac{f}{f_p} \right)^4 \exp \left[-af^2 \right] df + \int_{f_p}^{\infty} \exp \left[-af^2 \right] df} \quad (V-1)$$

The numerator of this expression can be written as follows:

$$\int_0^{\infty} \exp \left[-af^2 \right] df = \frac{\sqrt{2\pi}}{\sqrt{2a}} \int_0^{\infty} \frac{1}{\sqrt{2\pi}} \exp \left[-\frac{(\sqrt{2a} f)^2}{2} \right] \sqrt{2a} df.$$

This integral is the normal function and has a value of $1/2$.

$$\therefore \int_0^{\infty} \exp \left[-af^2 \right] df = \frac{\sqrt{\pi}}{2\sqrt{a}}. \quad (V-2)$$

The first integral in the denominator of (V-1) can be expanded through successive integration by parts into

$$- \left[f_p^2 + \frac{3}{2a} \right] \left[\frac{1}{2af_p^3} \right] \exp \left[-af_p^2 \right] + \frac{3}{[2af_p^2]^2} \int_0^{f_p} \exp \left[-af^2 \right] df.$$

The second integral in the denominator of (V-1) can be written as

$$\int_0^{\infty} \exp \left[-af^2 \right] df - \int_0^{f_p} \exp \left[-af^2 \right] df.$$

The left-hand integral has been evaluated above. The denominator of (V-1) can now be written as

$$\frac{\sqrt{\pi}}{2\sqrt{a}} - \left[f_p^2 + \frac{3}{2a} \right] \left[\frac{1}{2af_p^3} \right] \exp \left[-af_p^2 \right] + m \left[\frac{3}{(2af_p^2)^2} - 1 \right] \quad (V-3)$$

$$\text{where } m = \int_0^{f_p} \exp \left[-af^2 \right] df$$

m can be put in the form of the normal function by making the substitution $x = \sqrt{2a} f$ into the above integral.

$$\begin{aligned} \text{Then } \int_0^{f_p} \exp \left[-af^2 \right] df &= \frac{\sqrt{\pi}}{\sqrt{a}} \int_0^{\sqrt{2af_p}} \frac{1}{\sqrt{2\pi}} \exp \left[-\frac{x^2}{2} \right] dx \\ &= \frac{\sqrt{\pi}}{\sqrt{a}} n \\ \text{where } n &= \int_0^{\sqrt{2af_p}} \exp \left[-\frac{x^2}{2} \right] dx \text{ is the normal function.} \end{aligned}$$

Values for n as a function of the limits of the integral are given in many mathematical handbooks.*

* For example, Burington, R.S., op. cit. See Reference 7.

(V-3) is now written as

$$\frac{\sqrt{\pi}}{2\sqrt{a}} \left[1 + 2n \left(\frac{3b^2}{f_p^2} - 1 \right) \right] - b \left[1 + \frac{3b}{f_p} \right] \exp \left[-af_p^2 \right] \quad (V-4)$$

$$\text{where } b = \frac{1}{2af_p}.$$

Substituting (V-2) and (V-4) into (V-1),

$$R = \left\{ 1 - 2n + 6n \frac{b^2}{f_p^2} - \frac{2\sqrt{a}b}{\sqrt{\pi}} \left[1 + \frac{3b}{f_p} \right] \exp \left[-af_p^2 \right] \right\}^{-1} \quad (V-5)$$

Evaluation of this expression gives the attenuation of a Gaussian approximation to a clutter spectrum, when a 12-db-per-octave active high-pass filter is used. Consider the case when a filter having a cutoff frequency of 100 Hz attenuates the spectrum provided by a radar operating at 10 GHz observing a clutter target subjected to a wind having a velocity of 20 m.p.h.

Skolnik* gives a value of a for the conditions cited of 2.3×10^{-3} . The constants in (V-5) are now as follows:

$$f_p = 100 \text{ Hz}$$

$$a = 2.3 \times 10^{-3} \text{ sec}^2$$

$$n = \int_0^{\sqrt{2af_p}} \exp \left[-\frac{x^2}{2} \right] dx = 0.5$$

$$b = \frac{1}{2af_p} = 2.17.$$

Substituting these values into the last term of (V-5) reveals this term to have a magnitude of the order of 10^{-11} . This value is negligible compared to that of the $6n \frac{b^2}{f_p^2}$ term. Hence, if this term is disregarded, (V-5) can be written simply as

$$\left[6n \frac{b^2}{f_p^2} \right]^{-1}.$$

$$\text{Finally, } R = \frac{4a^2 f_p^4}{3}$$

$$= 705$$

$$= 28.5 \text{ db.}$$

* Skolnik, M.I., op. cit. See Reference 3.

REFERENCES

1. Kerr, D. E., Propagation of Short Radio Waves, pp 553-338, McGraw-Hill Book Company, Inc., New York (1951).
2. Barlow, E. J., "Doppler Radar," Proceedings of the IRE, Vol. 37, pp 340-355 (April 1949).
3. Skolnik, M. I., Introduction to Radar Systems, p 146, McGraw-Hill Book Company, Inc., New York (1962).
4. Davenport, W. B. and Root, W. R., Random Signals and Noise, Chapter 6, McGraw-Hill Book Company, Inc., New York (1958).
5. Lawson, J. L. and Uhlenback, G. E., Threshold Signals, pp 26-29, McGraw-Hill Book Company, Inc., New York (1950).
6. Hildebrande, F. B., Advanced Calculus for Applications, pp 80-91, Prentice-Hall, Inc., Englewood Cliffs (1964).
7. Burington, R. S., Handbook of Mathematical Tables and Formulas, Third Edition, p 88, Handbook Publishers, Inc., Sandusky (1954).
8. Gay, H. J., Analytic Geometry and Calculus, pp 156-159, McGraw-Hill Book Company, Inc., New York.

UNCLASSIFIED

Security Classification

DOCUMENT CONTROL DATA - R&D		
(Security classification of title, body of abstract and indexing annotation must be entered when the overall report is classified)		
1 ORIGINATING ACTIVITY (Corporate author) U. S. Army Electronics Command Fort Monmouth, New Jersey		2a REPORT SECURITY CLASSIFICATION UNCLASSIFIED
		2b GROUP
3 REPORT TITLE CLUTTER ATTENUATION ANALYSIS		
4 DESCRIPTIVE NOTES (Type of report and inclusive dates) Technical Report		
5 AUTHOR(S) (Last name, first name, initial) Fishbein, William Graveline, Stanley W. Rittenbach, Otto E.		
6 REPORT DATE March 1967	7a. TOTAL NO. OF PAGES 30	7b. NO. OF REFS 8
8a. CONTRACT OR GRANT NO.		9a. ORIGINATOR'S REPORT NUMBER(S) ECOM-2808
b. PROJECT NO. 1P6-20901-A-188		
c. Task No. 1P6-20901-A-188-03		9b. OTHER REPORT NO(S) (Any other numbers that may be assigned this report)
d. Subtask No. 1P6-20901-A-188-03-05		
10. AVAILABILITY/LIMITATION NOTICES Distribution of this document is unlimited.		
11. SUPPLEMENTARY NOTES		12. SPONSORING MILITARY ACTIVITY U. S. Army Electronics Command ATTN: AMSEL-HL-CT-R Fort Monmouth, N. J. 07703
13. ABSTRACT The performance of moving target indication (MTI) systems for combat surveillance radars depends to a large extent on the clutter spectrum, which is especially important when the radar attempts to detect slowly moving ground targets. This spectrum has long been assumed to be Gaussian shaped. However, MTI system performance predicted by this assumption was not achieved in practice. This report describes the results of an investigation conducted to determine the performance to be expected from an MTI system. The approach used was to measure the clutter rejection ratios afforded by various high-pass filters. The signal was taken from the boxcar demodulator of an X-band radar observing different clutter targets under varying wind conditions. Clutter rejection ratios of 10 to 40 db were measured. These results were then used to obtain a theoretical expression for the clutter power spectrum. This expression differs from the usual Gaussian assumption. Some credence is given to the results by a direct spectral analysis performed on a clutter signal. Two methods of filtering clutter signals which will result in acceptable MTI performance are suggested in this report. The results of this investigation are significant in that they have led to establishing criteria for a better MTI system design.		

14 KEY WORDS	LINK A		LINK B		LINK C	
	ROLE	WT	ROLE	WT	ROLE	WT
Radar MTI Moving Target Indication Clutter Clutter Filters Doppler Range-Gated Filters Video Processors						

INSTRUCTIONS	
<p>1. ORIGINATING ACTIVITY: Enter the name and address of the contractor, subcontractor, grantee, Department of Defense activity or other organization (<i>corporate author</i>) issuing the report.</p> <p>2a. REPORT SECURITY CLASSIFICATION: Enter the overall security classification of the report. Indicate whether "Restricted Data" is included. Marking is to be in accordance with appropriate security regulations.</p> <p>2b. GROUP: Automatic downgrading is specified in DoD Directive 5200.10 and Armed Forces Industrial Manual. Enter the group number. Also, when applicable, show that optional markings have been used for Group 3 and Group 4 as authorized.</p> <p>3. REPORT TITLE: Enter the complete report title in all capital letters. Titles in all cases should be unclassified. If a meaningful title cannot be selected without classification, show title classification in all capitals in parenthesis immediately following the title.</p> <p>4. DESCRIPTIVE NOTES: If appropriate, enter the type of report, e.g., interim, progress, summary, annual, or final. Give the inclusive dates when a specific reporting period is covered.</p> <p>5. AUTHOR(S): Enter the name(s) of author(s) as shown on or in the report. Enter last name, first name, middle initial. If military, show rank and branch of service. The name of the principal author is an absolute minimum requirement.</p> <p>6. REPORT DATE: Enter the date of the report as day, month, year, or month, year. If more than one date appears on the report, use date of publication.</p> <p>7a. TOTAL NUMBER OF PAGES: The total page count should follow normal pagination procedures, i.e., enter the number of pages containing information.</p> <p>7b. NUMBER OF REFERENCES: Enter the total number of references cited in the report.</p> <p>8a. CONTRACT OR GRANT NUMBER: If appropriate, enter the applicable number of the contract or grant under which the report was written.</p> <p>8b, 8c, & 8d. PROJECT NUMBER: Enter the appropriate military department identification, such as project number, subproject number, system numbers, task number, etc.</p> <p>9a. ORIGINATOR'S REPORT NUMBER(S): Enter the official report number by which the document will be identified and controlled by the originating activity. This number must be unique to this report.</p> <p>9b. OTHER REPORT NUMBER(S): If the report has been assigned any other report numbers (<i>either by the originator or by the sponsor</i>), also enter this number(s).</p>	<p>10. AVAILABILITY/LIMITATION NOTICES: Enter any limitations on further dissemination of the report, other than those imposed by security classification, using standard statements such as:</p> <p>(1) "Qualified requesters may obtain copies of this report from DDC."</p> <p>(2) "Foreign announcement and dissemination of this report by DDC is not authorized."</p> <p>(3) "U. S. Government agencies may obtain copies of this report directly from DDC. Other qualified DDC users shall request through _____."</p> <p>(4) "U. S. military agencies may obtain copies of this report directly from DDC. Other qualified users shall request through _____."</p> <p>(5) "All distribution of this report is controlled. Qualified DDC users shall request through _____."</p> <p>If the report has been furnished to the Office of Technical Services, Department of Commerce, for sale to the public, indicate this fact and enter the price, if known.</p> <p>11. SUPPLEMENTARY NOTES: Use for additional explanatory notes.</p> <p>12. SPONSORING MILITARY ACTIVITY: Enter the name of the departmental project office or laboratory sponsoring (<i>paying for</i>) the research and development. Include address.</p> <p>13. ABSTRACT: Enter an abstract giving a brief and factual summary of the document indicative of the report, even though it may also appear elsewhere in the body of the technical report. If additional space is required, a continuation sheet shall be attached.</p> <p>It is highly desirable that the abstract of classified reports be unclassified. Each paragraph of the abstract shall end with an indication of the military security classification of the information in the paragraph, represented as (TS), (S), (C), or (U).</p> <p>There is no limitation on the length of the abstract. However, the suggested length is from 150 to 225 words.</p> <p>14. KEY WORDS: Key words are technically meaningful terms or short phrases that characterize a report and may be used as index entries for cataloging the report. Key words must be selected so that no security classification is required. Identifiers, such as equipment model designation, trade name, military project code name, geographic location, may be used as key words but will be followed by an indication of technical context. The assignment of links, rules, and weights is optional.</p>